^{99m}Tc-3SPboroxime: A neutral ^{99m}Tc(III) radiotracer with high heart uptake and long myocardial retention

Xiao-Ying Xi, MD,[a] Lei Wang, MD,[a] Bailing Hsu, PhD,[b] Zuo-Quan Zhao, PhD,[a] Shuang Liu, PhD,[c] and Wei Fang, MD[a]

[a] Department of Nuclear Medicine, Fuwai Hospital, National Center for Cardiovascular Diseases, Chinese Academy of Medical Sciences and Peking Union Medical College, Beijing, China
[b] Nuclear Science and Engineering Institute, University of Missouri-Columbia, Columbia, MO
[c] School of Health Sciences, Purdue University, West Lafayette, IN

Received Oct 6, 2019; accepted Feb 24, 2020
doi:10.1007/s12350-020-02087-3

Background. **^{99m}Tc-3SPboroxime is a ^{99m}Tc(III) complex with high initial heart uptake comparable to that of ^{99m}Tc-Teboroxime, but with significantly longer myocardial retention in Sprague–Dawley rats. This study was performed to demonstrate its feasibility on myocardial perfusion imaging and myocardial blood flow quantification in swine models.**

Methods. **Dynamic single-photon emission computed tomography (SPECT) studies with ^{99m}Tc-3SPboroxime were performed in normal (with/without dipyridamole, n = 9) and acute myocardial infarction (AMI) swine (n = 3) in comparison with ^{99m}Tc-Teboroxime and ^{99m}Tc-Sestamibi. List-mode acquisitions were immediately started after injection and continued for 15 minutes. Regions of interest were drawn on heart (infarct and remote areas of AMI swine) and liver to generate time activity curves. Heart/liver and infarct/remote radioactivity ratios were calculated. One-tissue compartment model was implemented to obtain K_1 and K_2 values.**

Results. **The initial heart uptake of ^{99m}Tc-3SPboroxime was close to that of ^{99m}Tc-Teboroxime, but higher than that of ^{99m}Tc-Sestamibi. ^{99m}Tc-3SPboroxime had a myocardial retention longer than that of ^{99m}Tc-Teboroxime. The heart/liver ratio of ^{99m}Tc-3SPboroxime was higher than that of ^{99m}Tc-Teboroxime at later stage (13-15 minutes post-injection). The K_1 value of ^{99m}Tc-3SPboroxime was much higher than that of ^{99m}Tc-Sestamibi, and the K_2 value was significantly lower than that of ^{99m}Tc-Teboroxime both at rest and dipyridamole stress (rest K_1: 0.63 ± 0.11 vs 0.40 ± 0.04 mL·min^{-1}·g^{-1}, $P = 0.027$; stress K_1: 0.89 ± 0.05 vs 0.54 ± 0.08 mL·min^{-1}·g^{-1}, $P = 0.031$; rest K_2: 0.22 ± 0.04 vs 0.33 ± 0.11 mL·min^{-1}·g^{-1}, $P = 0.003$; stress K_2: 0.31 ± 0.03 vs 0.60 ± 0.30 mL·min^{-1}·g^{-1}, $P = 0.047$). High quality**

Electronic supplementary material The online version of this article (https://doi.org/10.1007/s12350-020-02087-3) contains supplementary material, which is available to authorized users.

The authors of this article have provided a PowerPoint file, available for download at SpringerLink, which summarizes the contents of the paper and is free for re-use at meetings and presentations. Search for the article DOI on SpringerLink.com.''

The authors have also provided an audio summary of the article, which is available to download as ESM, or to listen to via the JNC/ASNC Podcast.

Funding This study was supported by Chinese Academy of Medical Sciences Innovation Fund for Medical Sciences (2018-I2M-3-001), Grant 81771872 from the National Nature Science Foundation of China, and Purdue University, Grant R21 EB017237-01 from the National Institute of Biomedical Imaging and Bioengineering (NIBIB).

Reprint requests: Zuo-Quan Zhao, PhD, and Wei Fang, MD, Department of Nuclear Medicine, Fuwai Hospital, National Center for Cardiovascular Diseases, Chinese Academy of Medical Sciences and Peking Union Medical College, No. 167, North Lishi Road, Xicheng District, Beijing 100037, China; *418zhaozuoquan@163.com*, *nuclearfw@126.com*; and Shuang Liu, PhD, School of Health Sciences, Purdue University, 550 Stadium Mall 3 Drive, West Lafayette, IN 47907; *liu100@purdue.edu*

1071-3581/$34.00

Published online: 16 March 2020

SPECT images could be obtained in any of the 5 minutes windows over the first 15 minutes after injection of ^{99m}Tc-3SPboroxime in normal and AMI swine models. Apical and anterior perfusion defects were clearly visualized in AMI swine.

Conclusion. **^{99m}Tc-3SPboroxime is a promising radiotracer for future clinical translation considering its heart uptake, heart/liver ratio and SPECT image quality, as well as the advantage over ^{99m}Tc-Sestamibi in the definition of stress flow. (J Nucl Cardiol 2020)**

Key Words: ^{99m}Tc(III) radiotracer • SPECT • myocardial blood flow • acute myocardial infarction

Abbreviations	
CAD	Coronary artery disease
MBF	Myocardial blood flow
MPI	Myocardial perfusion imaging
SPECT	Single-photon emission computed tomography
AMI	Acute myocardial infarction
CZT	Cadmium zinc telluride
ROI	Region of interest
p.i.	Post-injection
PET	Positron emission tomography

INTRODUCTION

Coronary artery disease (CAD) is one of the leading causes of morbidity and mortality worldwide. The CAD arising from gradual narrowing of coronary arteries due to atherosclerotic deposits decreases myocardial blood flow (MBF). Myocardial perfusion imaging (MPI) with radiotracers can be utilized to evaluate myocardial perfusion and areas of perfusion defects noninvasively.[1-3] In order to accurately evaluate perfusion defects, the myocardial uptake of radiotracer must be proportional to MBF.[3-6] The biodistribution properties of an ideal radiotracer should be connected with the regional blood flow rather than receptor binding or metabolism. It should also have a high first-pass heart uptake to give a good linear relationship between heart uptake and regional blood flow with a stable myocardial retention, and a high tissue background ratio. A radiotracer with the decreased myocardial extraction can cause the ''roll-off'' phenomena in its heart uptake and leads to loss of linear relationship between its heart uptake and MBF.[4,5] ^{99m}Tc-Sestamibi as the most widely used radiotracer for MPI in nuclear cardiology encompasses a low first-pass extraction fraction and lacks of a linear relationship between its heart uptake and regional blood flow rates at > 2.5 mL·min^{-1}·g^{-1} [3,4] This shortcoming makes it challenging to accurately quantity MBF with ^{99m}Tc-Sestamibi.

^{99m}Tc-Teboroxime ([^{99m}TcCl(CDO)(CDOH)$_2$B-CH$_3$]; $CDOH_2$ = cyclohexanedione dioxime) is a member of the BATO (boronic acid adducts of technetium dioximes) class of neutral ^{99m}Tc(III) complexes. ^{99m}Tc-Teboroxime has a high first-pass extraction fraction and good linear relationship between its heart uptake and MBF, which is advantageous over ^{99m}Tc-Sestamibi and ^{99m}Tc-Tetrofosmin for MPI[7-9] However, early clinical experiences with ^{99m}Tc-Teboroxime were disappointing due to its rapid myocardial washout and low counting rate of standard single-photon emission computed tomography (SPECT) cameras[7,8]

To overcome the shortcomings associated with ^{99m}Tc-Teboroxime, a series of ^{99m}Tc(III) complexes [^{99m}TcL(CDO)(CDOH)$_2$B–R] (L = Cl, F, N_3 and SCN; R = alkyls or aryls) have been prepared and evaluated as heart imaging agents[10-13] The results showed that ^{99m}Tc-3SPboroxime ([^{99m}TcCl(CDO)(CDOH)$_2$B-3SP] 3SP-B(OH)$_2$ = 3-(methylsulfonyl)pyridineboronic acid) had an initial heart uptake close to that of ^{99m}Tc-Teboroxime, but with a significantly longer myocardial retention in Sprague–Dawley rats[14] Its tissue-to-background ratio and SPECT image quality were also better than that of ^{99m}Tc-Teboroxime in rats.

As a continuation of previous study, ^{99m}Tc-3SPboroxime was evaluated in normal and acute myocardial infarction (AMI) miniature swine models. Since ^{99m}Tc-Sestamibi and ^{99m}Tc-Teboroxime are the Food and Drug Administration approved radiotracers for MPI, biodistribution properties of ^{99m}Tc-3SPboroxime was compared with those of ^{99m}Tc-Teboroxime and ^{99m}Tc-Sestamibi in the same animal models. The main objective of this study was to demonstrate that ^{99m}Tc-3SPboroxime exhibits high first-pass extraction for MBF quantification and prolonged myocardial retention for standard MPI.

METHODS

Materials

Citric acid, γ-cyclodextrin, cyclohexanedione dioxime ($CDOH_2$), diethylenetriaminepentaacetic acid (DTPA), 3-(methylsulfonyl)pyridineboronic acid (3SP-B(OH)$_2$), sodium chloride, and $SnCl_2·2H_2O$ were purchased from Sigma/Aldrich (St. Louis, MO) or Matrix Scientific (Columbia, SC). Na^{99m}TcO$_4$ was obtained from HTA (Beijing, China). Cardiolite® vials was obtained from Shihong co. LTD (Beijing,

China). ^{99m}Tc-Sestamibi was prepared according to the manufacturer's package insert.

Radiosynthesis and Analytical Methods

^{99m}Tc-3SPboroxime and ^{99m}Tc-Teboroxime were prepared according to the literature procedure.[11-13] After radiolabeling, the reconstituted vial was cooled down to room temperature. A sample of the resulting solution was diluted with saline containing ~20% propylene glycol. The diluted solution was analyzed by high performance liquid chromatogram (HPLC) and instant thin layer chromatography (ITLC). The HPLC method for analysis of ^{99m}Tc-3SPboroxime and ^{99m}Tc-Teboroxime used an Agilent HP-1100 HPLC system (Agilent Technologies, Santa Clara, CA) equipped with a β-ram IN/US detector (Tampa, FL) and Zorbax C8 column (4.6 mm × 250 mm, 300 Å pore size; Agilent Technologies, Santa Clara, CA). The flow rate was 1 mL·min^{-1}. The mobile phase was isocratic with 30% solvent A (10 mM NH_4OAc buffer, pH 6.8) and 70% solvent B (methanol) between 0 and 5 minutes, followed by a gradient from 70% solvent B at 5 minutes to and 90% solvent B at 15 minutes and isocratic mobile phase with 10% solvent A and 90% solvent B. The radiochemical purity (RCP) is reported as the percentage of area for the expected peak on each HPLC. The ITLC used Gelman Sciences silica-gel strips and a 1:1 mixture of acetone and saline as the mobile phase. ^{99m}Tc-3SPboroxime, ^{99m}Tc-Teboroxime and $^{99m}TcO_4^-$ migrated to solvent front while [^{99m}Tc]colloid stayed at the origin. [^{99m}Tc]colloid was reported as the percentage of radioactivity at the origin over the total radioactivity on each strip. The RCP was > 95% with minimal [^{99m}Tc]colloid (< 0.5%) before being used for animal studies.

Doses Preparation

The kit solution was loaded onto a 0.22 μm syringe-driven filter, which was flushed with 0.5 mL of saline containing 50% propylene glycol that was used to prevent adsorption of ^{99m}Tc radiotracer on the surface of glass vial and syringe. For heart localization, ~ 37 MBq of radiotracer was pre-injected. The injection volume was ~ 3.0 mL per animal. Immediately after that, a dose of ~ 370 MBq radiotracer was injected for imaging studies. The injection volume was ~ 4.0 mL per animal.

Animal Preparation

All animal studies were performed under a protocol approved by Beijing Administration Office of Laboratory Animal (BAOLA). Healthy Chinese mini-swine (25–40 Kg) were obtained from Animal Center of Fuwai Hospital and were acclimated for > 24 hours. Animals were first fasted for 12 hours, and then anesthetized with intravenous injection of a mixture of ketamine (25 mg·kg^{-1}) and diazepam (1.1 mg·kg^{-1}) before being used for imaging studies. Anesthesia was supplemented as needed.

AMI was induced in 3 mini-swine (1 Female, 2 males; weight, 33–39 kg). The mini-swine were anesthetized as mentioned above. Right femoral artery and vein were exposed and isolated, and then a 7F introducer placed. The AMI model was induced with inflation of a balloon just distal to the first diagonal branch of the left anterior descending coronary artery. Complete occlusion was maintained by balloon dilatation for 120-150 minutes. Coronary occlusion was confirmed by coronary angiography. Electrocardiogram was performed at the baseline and after the surgery to confirm the success of the AMI animal model.

SPECT Imaging and Image Processing

SPECT studies were performed in 9 healthy and 3 AMI swine (30-40 kg). Dipyridamole stress SPECT scan was performed in 4 healthy swine (30-35 Kg). Healthy Chinese mini-swine were anesthetized and placed prone on the scanning table following a continuous intravenous infusion of dipyridamole (140 μg·kg^{-1}·min^{-1}) over 4 minutes prior to ^{99m}Tc radiotracers injection 3 minutes after the completion of dipyridamole infusion. The rest and stress SPECT scan were completed on 2 consecutive days.

Dynamic SPECT scans were acquired in list-mode data format on a Discovery NM 530c cadmium zinc telluride (CZT) SPECT camera (GE, USA) and followed by a CT scan on a GE Discovery 640 SPECT/CT camera. The animal was anesthetized, monitored with electrocardiogram (ECG), and kept in the same position. After localizing the heart, the animal was injected with ~ 370 MBq of ^{99m}Tc radiotracer. Injections of different radiotracers into the same swine were conducted on three consecutive days to avoid radioactive interference with ^{99m}Tc. List-mode acquisitions were immediately started and continued for 15 minutes. For SPECT image reconstruction, the list-mode data were rebinned to create dynamic raw data (15 frames; 1 minute per frame) and reconstructed with a dedicated SPECT processing software, MyoFlowQ (BCBTI, Taiwan). Quantitative dynamic images were then analyzed to measure with ImageJ 1.49 (the National Institutes of Health, United States) by an experienced nuclear medicine physician. The region of interest (ROI) for each swine was measured three times. For normal swine, the ROI was manually drawn on heart and liver at the same position. For AMI swine, the ROIs were drawn on the infarct and normal areas of the heart, respectively. The average radioactivity counts were recorded and time activity curves (TAC) were generated. For MBF quantitation, the list-mode data were rebinned to create dynamic raw data (22 frames; 10 sec × 10 frames + 20 sec × 5 frames + 60 sec × 7 frames) and reconstructed by the same software program. TAC of blood pool was measured in left ventricle and atrium region as TAC of myocardium was created by mapping myocardium in dynamic images into dynamic polar maps.

One-tissue compartment (two-compartment) kinetic model (Figure 1) was implemented for ^{99m}Tc radiotracers to fit three kinetic parameters by numeric optimization using the Levenberg–Marquardt method, including (K_1, K_2) transport coefficients, fractional blood volume (FBV) for blood pool spillover estimation, and (1-FBV) for partial volume correction to myocardial uptake as follows[15]:

$$C_{\mathrm{myo}}(t) = \mathrm{FBV} \cdot C_{\mathrm{a}}(t) + (1-\mathrm{FBV}) \cdot K_1 e^{-K_2 t} \otimes C_{\mathrm{a}}(t),$$

where $C_{\mathrm{myo}}(t)$ and $C_{\mathrm{a}}(t)$ are the measured activity concentrations in myocardium and blood pool for arterial input obtained from dynamic SPECT images, respectively. Prior to kinetic modeling, the dynamic polar map from early frame of myocardium before the incoming ^{99m}Tc radiotracer activity into the left heart region was analyzed with two volumes of interest placed in septal and lateral walls, respectively. Activity renormalization in septal wall region was performed by the threshold of activity in the lateral wall region to correct for the right ventricle spillover.

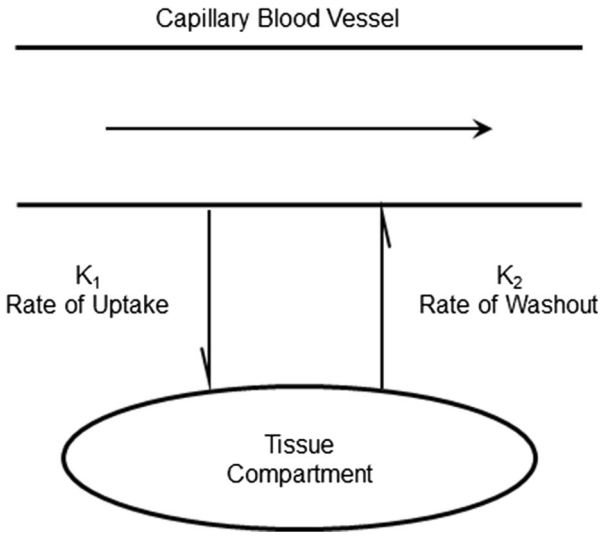

Figure 1. One-tissue compartment (two-compartment) kinetic model implemented for ^{99m}Tc-Teboroxime, ^{99m}Tc-Sestamibi and ^{99m}Tc-3SPboroxime.

Statistical Analysis

All quantitative data were expressed as the means ± standard deviation. Comparison between two radiotracers was made using a one-way ANOVA test. The level of significance was set at $P < 0.05$. The SPSS 19.0 software package (SPSS inc., Chicago, IL, USA) was used for statistical analyses.

RESULTS

Dynamic SPECT Imaging in Normal Swine

Figure 2 shows representative SPECT images of the normal mini-swine administered with ^{99m}Tc-Teboroxime, ^{99m}Tc-Sestamibi and ^{99m}Tc-3SPboroxime, respectively over the first 15 minutes post-injection (p.i.). ^{99m}Tc-Teboroxime had a fast myocardial washout kinetics within 8 minutes p.i., which was too short for conventional SPECT data acquisition. The heart uptake of ^{99m}Tc-Sestamibi was stable, but its liver uptake was higher than that of ^{99m}Tc-Teboroxime and ^{99m}Tc-3SPboroxime. Compared with ^{99m}Tc-Teboroxime, ^{99m}Tc-3SPboroxime exhibited a prolonged myocardial retention. Its liver radioactivity increased slowly, and seemed not yet to interfere with that in myocardium over the first 5 minutes p.i. As a result, high quality SPECT images could be obtained across a 15 minutes window.

Figure 3A compares the heart uptake of ^{99m}Tc-Teboroxime, ^{99m}Tc-Sestamibi and ^{99m}Tc-3SPboroxime over the 15 minutes period p.i. Although the initial heart

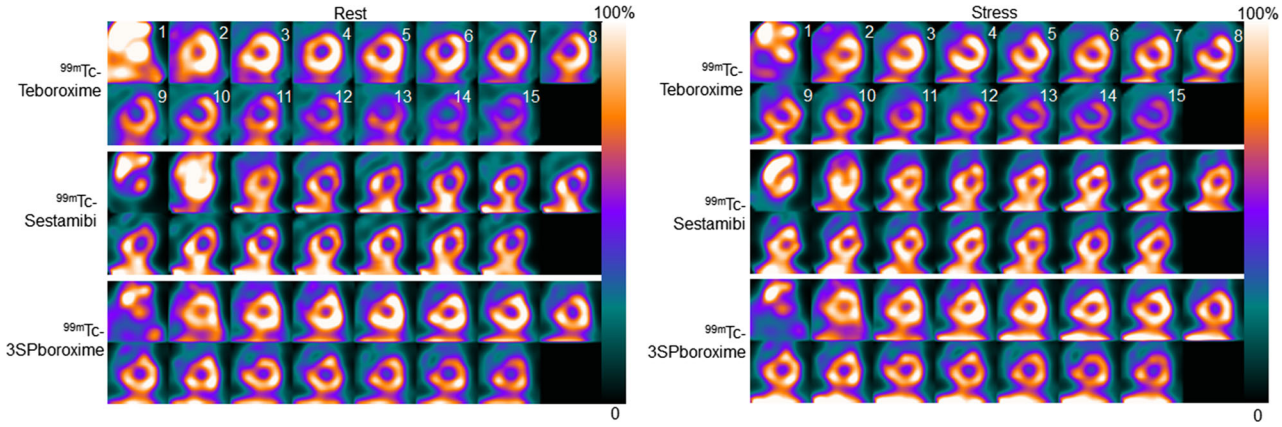

Figure 2. Representative short axis slice of SPECT images of the normal swine administered with ~ 370 MBq of ^{99m}Tc-Teboroxime, ^{99m}Tc-sestamibi and ^{99m}Tc-3SPboroxime at 0-15 minutes post-injection at rest and dipyridamole stress SPECT scan (1 picture per minute).

Table 1. R^2 values of ^{99m}Tc-Teboroxime, ^{99m}Tc-Sestamibi and ^{99m}Tc-3SPboroxime at rest and dipyridamole stress SPECT scan

Kinetic parameters	^{99m}Tc-Teboroxime	^{99m}Tc-Sestamibi	^{99m}Tc-3SPboroxime
Rest	0.91 ± 0.04*	0.88 ± 0.04	0.91 ± 0.01*
Stress	0.94 ± 0.02	0.90 ± 0.02	0.93 ± 0.02

Table 2. K_1 and K_2 values of ^{99m}Tc-Teboroxime, ^{99m}Tc-Sestamibi and ^{99m}Tc-3SPboroxime at rest and dipyridamole stress SPECT scan

SPECT protocol	Kinetic parameters ($mL \cdot min^{-1} g^{-1}$)	^{99m}Tc-Teboroxime	^{99m}Tc-Sestamibi	^{99m}Tc-3SPboroxime
Rest	K_1	0.69 ± 0.35*	0.40 ± 0.04	0.63 ± 0.11*
	K_2	0.33 ± 0.11*†	0.13 ± 0.03	0.22 ± 0.04*
Stress	K_1	1.26 ± 0.33*†	0.54 ± 0.08	0.89 ± 0.05*
	K_2	0.60 ± 0.30*†	0.16 ± 0.05	0.31 ± 0.03

*$P < 0.05$, ^{99m}Tc-Teboroxime or ^{99m}Tc-3SPboroxime vs ^{99m}Tc-Sestamibi
†$P < 0.05$, ^{99m}Tc-Teboroxime vs ^{99m}Tc-3SPboroxime

uptake of ^{99m}Tc-Teboroxime was slightly higher than that of ^{99m}Tc-3SPboroxime, it declined more rapidly after 4 minutes. Nonetheless, ^{99m}Tc-3SPboroxime and ^{99m}Tc-Teboroxime were able to share similar heart uptake over the first 10 minutes (all $P > 0.05$, Supplement Table 1). Beginning from 11 minutes to the end of the imaging, ^{99m}Tc-3SPboroxime gave a longer myocardial retention than that of ^{99m}Tc-Teboroxime (all $P < 0.05$, Supplement Table 1). The heart uptake of ^{99m}Tc-Sestamibi was stable and lower than that of ^{99m}Tc-3SPboroxime (all $P < 0.05$, Supplement Table 1).

The liver uptake values and heart/liver ratios for ^{99m}Tc-Teboroxime, ^{99m}Tc-Sestamibi and ^{99m}Tc-3SPboroxime are shown in Figure 3B and C, respectively. The initial liver uptake of ^{99m}Tc-Teboroxime and ^{99m}Tc-3SPboroxime was significantly lower than that of ^{99m}Tc-Sestamibi (all $P < 0.05$, Supplement Table 2). The heart/liver ratios of ^{99m}Tc-Teboroxime and ^{99m}Tc-3SPboroxime were higher than that of ^{99m}Tc-Sestamibi during the period of 1-8 minutes and 2-10 minutes p.i., respectively (all $P < 0.05$, Supplement Table 3). Since the heart uptake of ^{99m}Tc-Teboroxime decreased rapidly over time, its heart/liver ratio was much lower than that of ^{99m}Tc-3SPboroxime from 13 minutes p.i. to the end of imaging (all $P < 0.05$, Supplement Table 3).

Figure 4 shows the TAC for blood pool and myocardium after the injection of ^{99m}Tc-Teboroxime, ^{99m}Tc-Sestamibi and ^{99m}Tc-3SPboroxime at rest and dipyridamole stress dynamic scans. Initially, ^{99m}Tc-Sestamibi showed the highest peak in the blood pool TAC, middle for ^{99m}Tc-3SPboroxime and lowest for ^{99m}Tc-Teboroxime. After 10 minutes, blood pool activities of all three radiotracers decreased to a similar background level. For myocardium, rest and stress TACs of ^{99m}Tc-Teboroxime showed distinct climbs and then followed by rapid declines after 3 minutes. ^{99m}Tc-3SPboroxime demonstrated relatively slower climbs and declines as ^{99m}Tc-Sestamibi maintained relatively flat lines across 10 minutes. When the one-tissue compartment modeling was implemented to fit kinetic parameters (K_1, K_2) with blood pool and myocardial TACs, the square of correlation coefficient (R^2) was utilized to measure the level of model fit for three radiotracers. All of them were able to perform high $R^2 > 0.88$ for their rest and stress dynamic scans as listed in Table 1. Nonetheless, rest R^2 values of ^{99m}Tc-Teboroxime and ^{99m}Tc-3SPboroxime were significantly higher than that of ^{99m}Tc-Sestamibi (0.91 ± 0.04 vs 0.88 ± 0.04, $P = 0.018$; 0.91 ± 0.01 vs 0.88 ± 0.04, $P = 0.047$) and no difference for stress.

K_1 and K_2 values of ^{99m}Tc-Teboroxime, ^{99m}Tc-Sestamibi and ^{99m}Tc-3SPboroxime at rest and stress dynamic scans are listed in Table 2. The rest K_1 value of ^{99m}Tc-3SPboroxime was significantly higher than that of

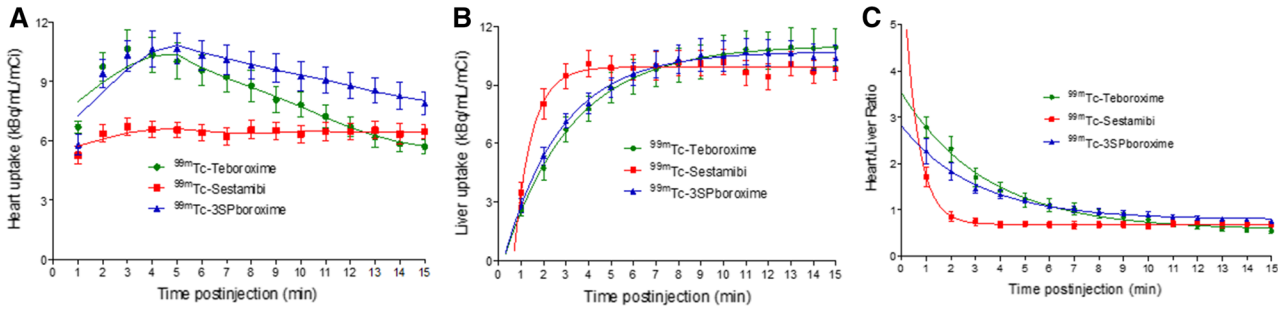

Figure 3. Comparison of heart uptake (**A**), liver uptake (**B**) and heart/liver ratios (**C**) between ^{99m}Tc-Teboroxime, ^{99m}Tc-sestamibi and ^{99m}Tc-3SPboroxime in normal swine. All experimental data were from dynamic SPECT image quantification in nine normal swine.

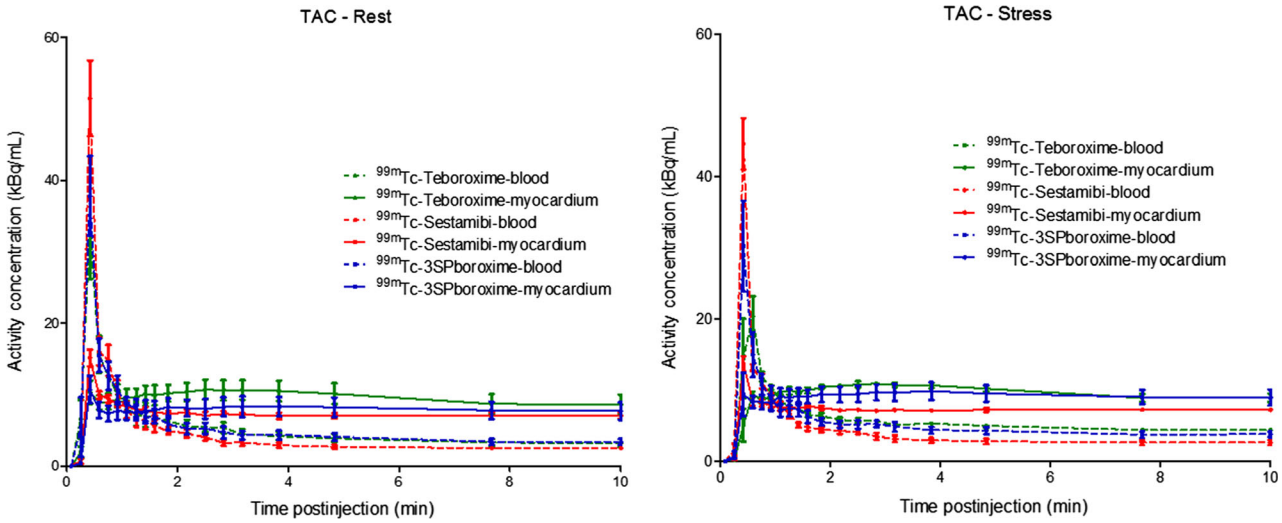

Figure 4. Time activity curves for blood and myocardium after the injection of ^{99m}Tc-Teboroxime, ^{99m}Tc-Sestamibi and ^{99m}Tc-3SPboroxime at rest and dipyridamole stress SPECT scan.

^{99m}Tc-Sestamibi (0.63 ± 0.11 vs 0.40 ± 0.04, $P = 0.027$). There was no difference in the K_1 values of ^{99m}Tc-3SPboroxime and ^{99m}Tc-Teboroxime (0.63 ± 0.11 vs 0.69 ± 0.35, $P = 0.584$). The K_2 value of ^{99m}Tc-3SPboroxime was significantly lower than that of ^{99m}Tc-Teboroxime (0.22 ± 0.04 vs 0.33 ± 0.11, $P = 0.003$), but higher than that of ^{99m}Tc-Sestamibi (0.22 ± 0.04 vs 0.13 ± 0.03, $P = 0.012$). For the dipyridamole stress dynamic scan, the K_1 value of ^{99m}Tc-3SPboroxime was significantly higher than that of ^{99m}Tc-Sestamibi (0.89 ± 0.05 vs 0.54 ± 0.08, $P = 0.031$), but lower than that of ^{99m}Tc-Teboroxime (0.89 ± 0.05 vs 1.26 ± 0.33, $P = 0.028$). The K_2 value of ^{99m}Tc-3SPboroxime was significantly lower than that of ^{99m}Tc-Teboroxime (0.31 ± 0.03 vs 0.60 ± 0.30, $P = 0.047$), and no difference with that of ^{99m}Tc-Sestamibi (0.31 ± 0.03 vs 0.16 ± 0.05, $P = 0.260$).

Dynamic SPECT Imaging in AMI Swine

Figures 5 and 6 show SPECT images and TACs of AMI swine over the first 15 minutes after administration of ^{99m}Tc-Teboroxime, ^{99m}Tc-Sestamibi and ^{99m}Tc-3SPboroxime, respectively. The myocardial uptake in the infarct area was significantly lower than that of the remote area. The apical and anterior perfusion defects were clearly visualized. High quality SPECT images were obtained during any of the 5 minutes windows over 15 minutes after injection of ^{99m}Tc-3SPboroxime. Because ^{99m}Tc-Teboroxime had a faster myocardial washout, the optimal image acquisition window could be limited to 0-5 minutes p.i.

The infarct/remote activity ratio was similar between ^{99m}Tc-3SPboroxime and ^{99m}Tc-Sestamibi, and no significant changes over 15 minutes p.i. Due to rapid

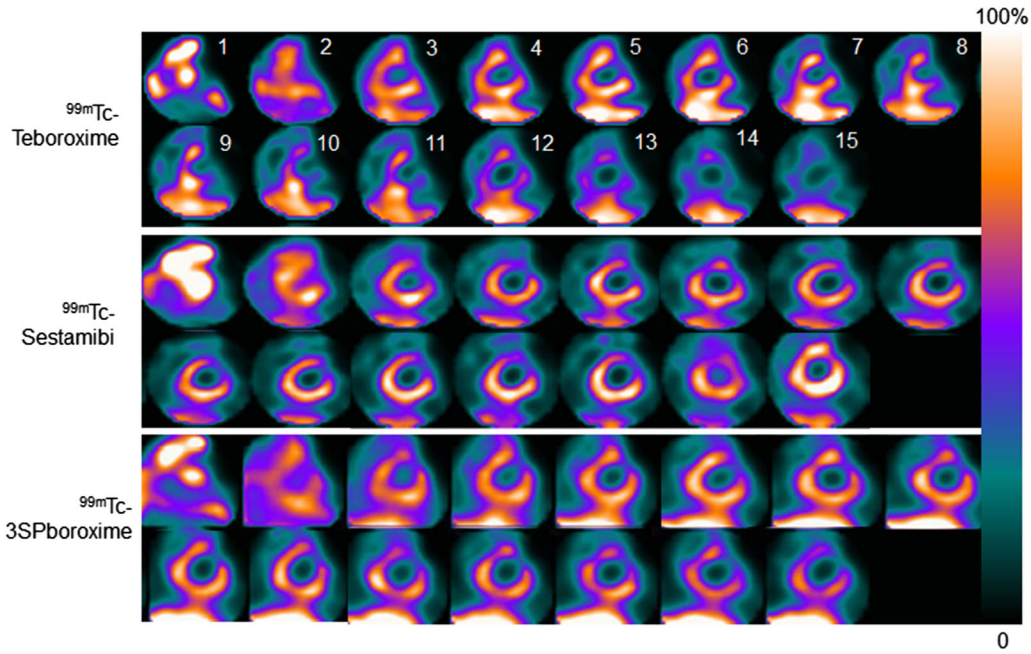

Figure 5. Representative short axis slice of SPECT images of the AMI swine administered with ~370 MBq of ^{99m}Tc-Teboroxime, ^{99m}Tc-Sestamibi and ^{99m}Tc-3SPboroxime at 0-15 min post-injection (1 picture per minute).

myocardial washout, the infarct/remote activity ratio of ^{99m}Tc-Teboroxime was increased and significantly higher than ^{99m}Tc-3SPboroxime and ^{99m}Tc-Sestamibi from 12 minutes p.i. (Figure 6, Supplement Table 4).

DISCUSSION

The main findings of this study were as followed: (1) the initial heart uptake of ^{99m}Tc-3SPboroxime was comparable to that of ^{99m}Tc-Teboroxime; (2) the K_1 value of ^{99m}Tc-3SPboroxime was significantly higher than that of ^{99m}Tc-Sestamibi, and the K_2 value was significantly lower than that of ^{99m}Tc-Teboroxime both at rest and dipyridamole stress; (3) high quality SPECT images could be obtained in any of the 5 minutes windows over the first 15 minutes after injection of ^{99m}Tc-3SPboroxime both in normal and AMI swine models.

Positron emission tomography (PET) MBF quantification has been clinically marked as a powerful tool for diagnosis and prognosis of CAD, its utilization as a clinical tool has several practical challenges, including commercial accessibility of PET radiotracers (^{15}O-water, ^{13}N-ammonia or, more recently ^{18}F-Flurpiridaz),[16-18] and high cost of radionuclide production facility, which are currently restricted to North America and Europe. Thus, SPECT MBF quantitation with the newly developed radiotracer might be a good solution to overcome the challenges associated with PET.

Recently, feasibility studies with ^{99m}Tc-Sestamibi and ^{99m}Tc-Tetrofosmin using standard and CZT-based SPECT cameras have shown great potential to expand quantification of the absolute blood flow and flow reserve into the SPECT field.[4-6,19] However, due to the ''roll-off'' phenomenon associated with ^{99m}Tc-Sestamibi and ^{99m}Tc-Tetrofosmin at higher blood flow rate, a proper physiological compensation for the non-linear relation between radiotracer uptake and MBF is required. Imaging errors in converting K_1 to MBF may be amplified post the correction. ^{99m}Tc-Teboroxime is a radiotracer with a first-pass extraction fraction higher than that of ^{99m}Tc-Sestamibi.[9,20] In this study, ^{99m}Tc-3SPboroxime was evaluated in swine and showed the initial heart uptake well comparable to that of ^{99m}Tc-Teboroxime, and much higher than that of ^{99m}Tc-Sestamibi. The myocardial retention of ^{99m}Tc-3SPboroxime was significantly longer than that of ^{99m}Tc-Teboroxime (Figures 2 and 3). This advantage enables a wider image acquisition window for perfusion imaging and maintain the accuracy for MBF quantitation with dynamic SPECT.

Kinetic modeling, a common technique to simplify physiological process, regularly utilizes two or three compartments to describe the radiotracer exchange between the blood and myocyte. The R^2 value of the

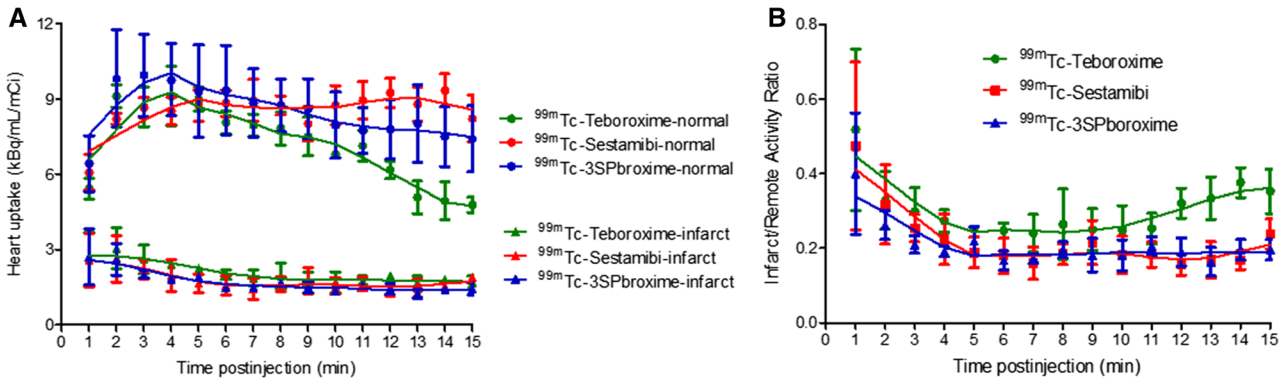

Figure 6. Comparison of heart uptake of ^{99m}Tc-Teboroxime, ^{99m}Tc-Sestamibi and ^{99m}Tc-3SPboroxime in infarct and remote area in AMI swine (**A**). Comparison of infarct/remote activity ratios of ^{99m}Tc-Teboroxime, ^{99m}Tc-Sestamibi and ^{99m}Tc-3SPboroxime (**B**). All experimental data were from dynamic SPECT image quantification in three AMI swine.

three radiotracers evaluated in this study were all high enough both at rest and dipyridamole stress, which verified the feasibility of one-tissue compartment model. ^{99m}Tc-Teboroxime revealed significantly higher K_1 and K_2 values than that of ^{99m}Tc-Sestamibi at both rest and dipyridamole stress (Table 2), which is consistent with the results from pre-clinical animal models,[20,21] and clinical studies in normal human subjects and patients.[22,23] The K_1 value of ^{99m}Tc-3SPboroxime was significantly higher than that of ^{99m}Tc-Sestamibi, suggesting its higher first-pass extraction fraction. Meanwhile, its K_2 value was significantly lower than that of ^{99m}Tc-Teboroxime, indicating a longer myocardial retention time for ^{99m}Tc-3SPboroxime. These two unique properties offer great clinical significance in identifying the ischemia, defining the extent and severity of heart disease, establishing the need for medical intervention, and monitoring the treatment effects in CAD patients.[4-6,24]

Both cellular and mitochondrial membranes are composed of phospholipid bilayers. Thus, the penetration of ^{99m}Tc radiotracers across cellular and mitochondrial membrane is most likely be the key to control myocardial uptake kinetics. Myocardium has the highest mitochondrial density due to their high metabolic activity, and may occupy up to 40% of total volume of myocytes. Other organs that rich in mitochondria include liver and spleen because of their excretory function. This might explain why ^{99m}Tc-Teboroxime and ^{99m}Tc-3SPboroxime tend to have very high uptake in the heart, liver and spleen.[10-14,25] Because of their neutrality, ^{99m}Tc-Teboroxime and ^{99m}Tc-3SPboroxime can penetrate with ease through cellular and mitochondrial membranes. It is not surprising that ^{99m}Tc-Teboroxime and ^{99m}Tc-3SPboroxime have high first-pass extraction fraction. In contrast, ^{99m}Tc-Sestamibi is cationic. The positive charge of ^{99m}Tc-Sestamibi is responsible for its stable myocardial uptake because of the negative mitochondrial potential. However, the extra positive charge makes it difficult for them to penetrate the highly packed mitochondrial membranes.[26,27] This might explain why ^{99m}Tc-Sestamibi has a long myocardial retention with relatively low first-pass extraction fraction.[10-14,25]

One might ask why ^{99m}Tc-3SPboroxime has a myocardial retention significantly longer than ^{99m}Tc-Teboroxime. One possible explanation is related to their cellular binding properties. Studies on the interaction of ^{99m}Tc-Teboroxime with liposomes indicated that it may bind to the membranes via its oximes by hydrogen-bonding or nonspecific adsorption to the hydrophilic head groups of myocyte cellular membranes.[7,8] However, the 3-methylsulfonyl group in ^{99m}Tc-3SPboroxime may play a significant role in their binding to cellular membranes. For ^{99m}Tc-Teboroxime, R is the methyl group, which has very limited interaction with the lipophilic fatty acid chain. For ^{99m}Tc-3SPboroxime, however, the 3-methylsulfonyl group is expected to form strong hydrogen bonds with the hydrophilic phosphate moieties in the lipid layer. The hydrogen-binding capability of the 3-methylsulfonyl group would afford a stronger interaction with the myocyte cellular membranes, which would lead to a slower dissociation rate and a longer myocardial retention time for ^{99m}Tc-3SPboroxime than that of ^{99m}Tc-Teboroxime.

The liver uptake of ^{99m}Tc-3SPboroxime was significantly lower than that of ^{99m}Tc-Sestamibi from 2 to 4 minutes p.i. Its heart/liver ratio was significantly higher than that of ^{99m}Tc-Sestamibi from 2 to 10 minutes p.i. High initial heart uptake and high heart/liver

ratios are important because dynamic imaging is often performed during the first 10-15 minutes after injection for conventional SPECT quantification of MBF. It also provides the capability to produce perfusion images with good quality. The SPECT images of ^{99m}Tc-3SPboroxime in both normal and AMI swine confirmed this feasibility as the left ventricular wall was clearly delineated and the apical and anterior perfusion defects were clearly visualized.

Limitations

This work has several limitations. Firstly, as lack of a gold standard measurement of blood flow (e.g., microspheres or perfusion PET), the difference between three radiotracers in quantification of blood flow can only be indirectly verified through comparison of K values. Previously, the comparison of K_1 to measure quantitative MBF among three commonly utilized SPECT radiotracers (^{99m}Tc-Sestamibi, ^{99m}Tc-Tetrofosmin, ^{201}Tl) was reported.[28] The work adopted microspheres as the good standard and concluded the higher K_1 represented closer to the true MBF under the same level of MBF as the relationship between K_1 and MBF can be described by the Renkin–Crone model. In our study, due to lack of resources to conduct the same experiment with radioactive microspheres, we chose to compare K_1 among ^{99m}Tc-Teboroxime, ^{99m}Tc-Sestamibi and ^{99m}Tc-3SPboroxime based on the observed relationship between K_1 and true MBF for SPECT radiotracers. Although indirect comparison may encompass the limitation, but K_1 itself is still able to expound the flow characteristic among different radiotracers in our study. Secondly, MPI and CT images were acquired using separate camera systems as the 530c CZT SPECT camera doesn't contain a CT scanner; therefore, positioning for the swine can't be completely identical which can affect attenuation correction. However, possible variation in swine positioning between and SPET and CT imaging was appropriately corrected by the software approach based on previous study.[29] Thirdly, different radiotracers were injected into the swine on three consecutive days to avoid radioactive interference with ^{99m}Tc. In AMI swine, myocardial perfusion may vary during this time gap due to myocardial edema and collateral circulation formation.

CONCLUSION

In this study, the combination of high heart uptake and long myocardial retention at rest and stress in both normal and AMI swine models suggested that ^{99m}Tc-3SPboroxime encompassed a wider time window to maintain high quality image with a better linear relationship between its heart uptake and regional myocardial blood flow. This unique characteristic is important for accurate quantification of regional MBF particularly under stress conditions, which has been considered challenging with ^{99m}Tc-Sestamibi.

NEW KNOWLEDGE GAINED

^{99m}Tc-3SPboroxime, a novel ^{99m}Tc labeled boronic acid derivative, with longer myocardial retention than that of ^{99m}Tc-Teboroxime while maintaining the high first-pass extraction fraction, is an excellent candidate for MPI and MBF quantification in future clinical translational study.

Disclosures

Xiao-Ying Xi, Lei Wang, Baling Hsu, Zuo-Quan Zhao, Shuang Liu and Wei Fang have nothing to disclose.

References

1. Henneman MM, Schuijf JD, van der Wall EE, Bax JJ. Non-invasive anatomical and functional imaging for the detection of coronary artery disease. Br Med Bull 2006;79–80:187–202.
2. Di Carli MF, Hachamovitch R. New technology for noninvasive evaluation of coronary artery disease. Circulation 2007;115:1464–80.
3. Baggish AL, Boucher CA. Radiopharmaceutical agents for myocardial perfusion imaging. Circulation 2008;118:1668–74.
4. Slomka PJ, Berman DS, Germano G. Absolute myocardial blood flow quantification with SPECT/CT: Is it possible? J Nucl Cardiol 2014;21:1092–5.
5. Klein R, Hung GU, Wu TC, Huang WS, Li D, deKemp RA, et al. Feasibility and operator variability of myocardial blood flow and reserve measurements with ^{99m}Tc-sestamibi quantitative dynamic SPECT/CT imaging. J Nucl Cardiol 2014;21:1075–88.
6. Nekolla SG, Rischpler C, Nakajima K. Myocardial blood flow quantification with SPECT and conventional tracers: A critical appraisal. J Nucl Cardiol 2014;21:1089–91.
7. Rumsey WL, Rosenspire KC, Nunn AD. Myocardial extraction of teboroxime: Effects of teboroxime interaction with blood. J Nucl Med 1992;33:94–101.
8. Marshall RC, Leidholdt EM Jr, Zhang DY, Barnett CA. The effect of flow on technetium-99m-teboroxime (SQ30217) and thallium-201 extraction and retention in rabbit heart. J Nucl Med 1991;32:1979–88.
9. Beanlands R, Muzik O, Nguyen N, Petry N, Schwaiger M. The relationship between myocardial retention of technetium-99m teboroxime and myocardial blood flow. J Am Coll Cardiol 1992;20:712–9.
10. Zheng Y, Ji S, Tomaselli E, Ernest C, Freiji T, Liu S. Effect of co-ligands on chemical and biological properties of ^{99m}Tc(III) complexes [^{99m}Tc(L)(CDO)(CDOH)$_2$BMe] (L = Cl, F, SCN and N_3; $CDOH_2$ = cyclohexanedione dioxime). Nucl Med Biol 2014;41:813–24.
11. Yang Y, Zheng Y, Tomaselli E, Fang W, Liu S. Impact of boronate capping groups on biological characteristics of novel

^{99m}Tc(III) complexes [^{99m}TcCl(CDO)(CDOH)$_2$B-R] ($CDOH_2$ = cyclohexanedione dioxime). Bioconjug Chem 2015;26:316–28.
12. Liu M, Zheng Y, Avcibasi U, Liu S. Novel ^{99m}Tc(III)-azide complexes [^{99m}Tc(N_3)(CDO)(CDOH)$_2$B-R] ($CDOH_2$ = cyclohexanedione dioxime) as potential radiotracers for heart imaging. Nucl Med Biol 2016;43:732–41.
13. Liu M, Fang W, Liu S. Novel ^{99m}Tc(III) complexes [^{99m}TcCl(CDO)(CDOH)$_2$B-R] ($CDOH_2$ = cyclohexanedione dioxime) useful as radiotracers for heart imaging. Bioconjug Chem 2016;27:2770–9.
14. Zhao ZQ, Liu M, Fang W, Liu S. Sulfonyl-containing boronate caps for optimization of biological properties of ^{99m}Tc(III) radiotracers [^{99m}TcCl(CDO)(CDOH)$_2$B–R]($CDOH_2$ = cyclohexanedione dioxime). J Med Chem 2018;61:319–28.
15. Klein R, Beanlands RS, deKemp RA. Quantification of myocardial blood flow and flow reserve: Technical aspects. J Nucl Cardiol 2010;17:555–70.
16. Danad I, Uusitalo V, Kero T, Saraste A, Raijmakers PG, Lammertsma AA, et al. Quantitative assessment of myocardial perfusion in the detection of significant coronary artery disease: Cutoff values and diagnostic accuracy of quantitative [^{15}O]H_2O PET Imaging. J Am Coll Cardiol 2014;64:1464–75.
17. Schindler TH. Positron-emitting myocardial blood flow tracers and clinical potential. Prog Cardiovasc Dis 2015;57:588–606.
18. Berman DS, Maddahi J, Tamarappoo BK, Czernin J, Taillefer R, Udelson JE, et al. Phase II safety and clinical comparison with single-photon emission computed tomography myocardial perfusion imaging for detection of coronary artery disease: Flurpiridaz F 18 positron emission tomography. J Am Coll Cardiol 2013;61:469–77.
19. Agostini D, Roule V, Nganoa C, Roth N, Baavour R, Parienti JJ, et al. First validation of myocardial flow reserve assessed by dynamic ^{99m}Tc-sestamibi CZT-SPECT camera: Head to head comparison with ^{15}O-water PET and fractional flow reserve in patients with suspected coronary artery disease: The WATERDAY study. Eur J Nucl Med Mol Imaging 2018;45:1079–90.
20. Smith AM, Gullberg GT, Christian PE. Experimental verification of technetium 99m-labeled teboroxime kinetic parameters in the myocardium with dynamic single-photon emission computed tomography: Reproducibility, correlation to flow, and susceptibility to extravascular contamination. J Nucl Cardiol 1996;3:130–42.
21. Meerdink DJ, Leppo JA. Experimental studies of the physiologic properties of technetium-99m agents: Myocardial transport of perfusion imaging agents. Am J Cardiol 1990;66:9E–15E.
22. Tartagni F, Fallani F, Corbelli C, Monetti N, Piovaccari G, Marzocchi A, et al. Dynamic planar myocardial perfusion imaging in patients with one-vessel disease with intracoronary injection of technetium 99m teboroxime during papaverine-induced coronary hyperemia. Am Heart J 1996;132:1042–7.
23. Burns RJ, Iles S, Fung AY, Wright LM, Daigneault L. The Canadian exercise technetium 99m-labeled teboroxime single-photon emission computed tomographic study. J Nucl Cardiol 1995;2:117–25.
24. Heo R, Nakazato R, Kalra D, Min JK. Noninvasive imaging in coronary artery disease. Semin Nucl Med 2014;44:398–409.
25. Liu M, Liu S. ^{99m}Tc-3Cboroxime: A novel ^{99m}Tc(iii) (III) complex[^{99m}TcCl(CDO)(CDOH)$_2$B-3C] ($CDOH_2$ = cyclohexanedione dioxime; 3C-$B(OH)_2$ = 3-(carbamoylphenyl)boronic acid) with high heart uptake and long myocardial retention. Dalton Trans 2017;46:14509–18.
26. Younès A, Songadele JA, Maublant J, Platts E, Pickett R, Veyre A. Mechanism of uptake of technetium-tetrofosmin. II: Uptake into isolated adult rat heart mitochondria. J Nucl Cardiol 1995;2:327–33.
27. Zhou Y, Liu S. ^{64}Cu-Labeled phosphonium cation as PET radiotracers for tumor imaging. Bioconjug Chem 2011;22:1459–72.
28. Wells RG, Timmins R, Klein R, Lockwood J, Marvin B, deKemp RA, et al. Dynamic SPECT measurement of absolute myocardial blood flow in a porcine model. J Nucl Med 2014;55:1685–91.
29. Wang L, Wu D, Yang Y, Chen IJ, Lin CY, Hsu B, et al. Avoiding full corrections in dynamic SPECT images impacts the performance of SPECT myocardial blood flow quantitation. J Nucl Cardiol 2017;24:1332–46.